Rigid Body Sampling and Boundary Handling for Rigid-Fluid Coupling of Particle Based Fluids

Xiaokun Wang, XiaoJuan Ban(✉), YaLan Zhang, and Xu Liu

University Science and Technology Beijing,
Beijing 100083, People's Republic of China
{wanglxiao2kun3,xuliu213}@163.com, banxj@ustb.edu.cn,
602980797@qq.com

Abstract. We propose an efficient and simple rigid-fluid coupling scheme employing rigid surface sampling and boundary handling for particle-based fluid simulation. This approach samples rigid bodies to boundary particles which are used for interacting with fluids. It contains two steps, sampling and relaxation, which guarantees uniform distribution of particles using less iterations. We integrate our approach into SPH fluids and implement several scenarios of rigid-fluid interaction. The experimental results demonstrate that our method is capable to implement interaction of rigid body and fluids while mainly ensuring physical authenticity for rigid-fluid coupling simulation.

Keywords: Physically-based simulation · Surface sampling · Boundary handling · Rigid-fluid coupling

1 Introduction

Physically-based fluid simulation is a popular issue in computer graphics while has a huge research and application demand in virtual reality. Two major schemes are used for animating fluids, the grid-based Eulerian approach and particle-based Lagrangian approach. Eulerian method is particularly suited to simulate large volumes fluid, but it is restricted by time step and computing time for small scale features. In contrast, Lagrangian method are suitable for capturing small scale effects such as spindrift, droplet. Among various Lagrangian approaches, Smoothed Particle Hydrodynamics (SPH) is the most popular method for simulating fluid due to computational simplicity and efficient.

In reality, rigid-fluid interaction widely exists in many scenarios. As a result, the interesting fluid behavior emerges when rigid objects are added to fluid simulation. While coupling of particle-based fluids with rigid objects seems to be straightforward, there are still several issues not well resolved. For one thing, rigid bodies must be sampled to particles in order to interact with particle-based fluids, but only a few rigid boundary sampling methods can be directly employed in rigid-fluid coupling simulation. For another thing, boundary handling method for rigid-fluid coupling is considerable. To cope with the increasing demand for more detailed fluids, we present

Y. Luo (Ed.): CDVE 2016, LNCS 9929, pp. 210–218, 2016.
DOI: 10.1007/978-3-319-46771-9_28

integrate rigid sampling and boundary for rigid-fluid coupling and design a practical and easy animation simulation scheme of rigid-fluid interaction.

2 Related Work

Monaghan's simulating free surface flows with SPH [1] serves as a basis for SPH fluid simulation. Muller et al. [2] proposed using gas state equation with surface tension and viscosity forces for interactive applications, which also bring compressibility issue. Becker et al. [3] proposed WCSPH which reduces compressibility with Tait Equation. It significantly increased realistic effects but the efficiency is limited by time step. As incompressibility is time-consuming, many improved algorithms were addressed to enhance the efficiency. Solenthaler et al. presented PCISPH [4] using a prediction-correction scheme which significantly improved efficiency. Ihmsen et al. addressed IISPH [5], which carefully constructs pressure poisson equation and solves it using Relaxed Jacobi, which has a great improvement in stability and convergence speed. Recently, Bender and Koschier [6] proposed a promising approach for impressible SPH. It combines two pressure solvers which enforces low volume compression and a divergence-free velocity field. It allows larger time steps which yields a considerable performance gain since particle neighborhoods updated less frequently.

For boundary handling and rigid-fluid coupling, distance-based penalty methods with boundary particles have been commonly used [7, 8]. However, these approaches require large penalty forces that restrict the time step meanwhile particles tend to stick to the boundary due to the lack of fluid neighbors. The sticking of particles is avoided with frozen and ghost particles based models [9]. In order to ensure non-penetration, the positions of penetrating particles should be corrected [10]. However, handling two-way interaction is problematic in these approaches since the elevated density on one side of a boundary particle affects potential fluid particles on the other side. For this reason, Ghost SPH scheme [11] resolves this with a narrow layer of ghost particles and Akinci et al. employed boundary particles to correct the calculation of fluid density [12]. Due to Ghost SPH is time-consuming, we employ Akinci's boundary handling method which is simple and easy to achieve in this paper.

For rigid surface sampling, Turk used repelling particles on surfaces to uniformly resample a static surface [13]. Witkin and Heckbert employed local repulsion to make particles spread uniform [14]. Cook addressed stochastic sampling of Poisson-disk distributions with blue noise [15]. Blue sampling has the ability to generate random points and get uniform distribution of sampling points. Hence, the following sampling methods always have blue noise characteristics. Corsini et al. sampled triangular meshes with blue noise [16]. Dunbar et al. [17] modified Poisson-disk sample using a spatial data structure. Bridson [18] simplified Dunbar's approach with rejection sampling and extending it to higher dimensions. Then Schechter [11] modified Bridson's approach and employed it to Ghost SPH. Inspired by Schechter's approach, we address a sampling method which is more efficient and easy to implement.

3 Particle-Based Fluid Simulation Framework

In the Lagrangian description, flow controlled equations of Navier-Stokes for fluids can be expressed as

$$\frac{d\rho_i}{dt} = -\rho_i \nabla \cdot v_i \tag{1}$$

$$\rho_i \frac{D\mathbf{v}_i}{Dt} = -\nabla p_i + \rho_i g + \mu \nabla^2 \mathbf{v}_i \tag{2}$$

Where $\mathbf{v}_i$ is the velocity, ρ_i is the density, p_i is the pressure, μ is the viscosity coefficient and g represents the external force field. Eq. (1) is mass equation and Eq. (2) momentum equation.

The SPH theory is to utilize the form of discrete particles to characterize the successive fields and use integration to approximate the fields. For particle i at location $\boldsymbol{x}_i$,

$$\langle A(\boldsymbol{x}_i) \rangle = \sum_j m_j \frac{A_j}{\rho_j} W\left(\boldsymbol{x}_i - \boldsymbol{x}_j, h\right) \tag{3}$$

Where m_j and ρ_j represent particle mass and density respectively, $W\left(\boldsymbol{x}_i - \boldsymbol{x}_j, h\right)$ is the smoothing kernel and h the smoothing radius.

Applying Eq. (3) to the density of a particle i at location $\boldsymbol{x}_i$ yields the summation of density

$$\rho_i = \sum_j m_j W\left(\boldsymbol{x}_i - \boldsymbol{x}_j, h\right) \tag{4}$$

Thus, forces between particles including pressure $\mathbf{f}_i^p$ and viscous force $\mathbf{f}_i^v$ can be represented as

$$\mathbf{f}_i^p = -\sum_j m_j \left(\frac{p_i}{\rho_i^2} + \frac{p_j}{\rho_j^2} \right) \nabla W_{ij} \tag{5}$$

$$\mathbf{f}_i^v = \mu \sum_j m_j \frac{\mathbf{v}_{ji}}{\rho_j} \nabla^2 W_{ij} \tag{6}$$

In this article, we employ Tait equation [3] to calculate the pressure and use the method in literature [12] to compute viscous force.

4 Boundary Handling for Particle-Based Fluids

Considering influence of boundary particles, density formula of fluid particles in (4) need to introduce weighted summation influence of boundary particle [12], that is

$$\rho_{f_i} = \sum_j m_{f_j} W_{ij} + \sum_k m_{b_k} W_{ik} \tag{7}$$

Where f_j, b_k denotes fluid particle j and boundary particle k respectively. This formula can overcome boundary defects in SPH fluid simulation to some extent.

The density of fluid particles is incorrect and instability when the setting of boundary particle mass is unreasonable or distribution of boundary particles is uneven. Hence, using the contribution of boundary particles to a fluid particle through taking the volume of boundary particles into account as

$$\Psi_{b_i}(\rho_0) = \rho_0 V_{b_i} \tag{8}$$

With ρ_0 denotes rest density of fluid, V_{b_i} is the estimation value of boundary area volume of corresponding boundary particles. Applying $\Psi_{b_i}(\rho_0)$ replace the boundary particle mass can guarantee the stability.

Therefore, Eq. (7) can be written as

$$\rho_{f_i} = \sum_j m_{f_j} W_{ij} + \sum_k \Psi_{b_k}(\rho_{0i}) W_{ik} \tag{9}$$

The pressure acceleration generated by boundary particles to fluid particles is

$$\frac{dv_{f_i}}{dt} = -\frac{kp_{f_i}}{\rho_{f_i}^2} \sum_k \Psi_{b_k}(\rho_{0i}) \nabla W_{ik} \tag{10}$$

Where $p_{f_i} > 0$ takes $k = 2$. When $p_{f_i} < 0$, boundary particles and fluid particles attract each other, then we can adjust parameter $k(0 \leq k \leq 2)$ to realize different adsorption effects, we choose $k = 1$ in our experiment.

To simulate the friction between fluid and rigid body, we have to compute the friction between boundary particles and fluid particles. The friction consults from artificial viscosity, that is

$$\frac{d\boldsymbol{v}_{f_i}}{dt} = -\sum_k \Psi_{b_k}(\rho_{0i}) \Pi_{ik} \nabla W_{ik} \tag{11}$$

Where $\Pi_{ik} = -\nu\left(\frac{\boldsymbol{v}_{ik}^T \boldsymbol{x}_{ik}}{\boldsymbol{x}_{ik}^2 + \varepsilon h^2}\right)$, $\nu = \frac{2\alpha h c_s}{\rho_k + \rho_j}$.

Then we can get the forces of boundary particles using Newton's third law. The forces generated by fluid particles to boundary particles is

$$\boldsymbol{F}_{b_k} = \sum_i \left(\frac{kp_{f_i}}{\rho_{f_i}^2} + \prod_{ik}\right) m_{f_i} \Psi_{b_k}(\rho_{0i}) \nabla W_{ik} \tag{12}$$

where i denotes the fluid neighbors of boundary particle k. It is the counter-acting force of Eqs. 10 and 11.

For a rigid body, the total force and torque need to be calculated. It can be separately written as

$$\boldsymbol{F}_{rigid} = \sum_k \boldsymbol{F}_{b_k} \tag{13}$$

$$\tau_{rigid} = \sum_k \left(\boldsymbol{x}_k - \boldsymbol{x}_{rigid}^{cm}\right) \times \boldsymbol{F}_{b_k} \tag{14}$$

Where $\boldsymbol{x}_k$ denotes the location of boundary particle k, $\boldsymbol{x}_{rigid}^{cm}$ is the mass center of a rigid body. The total force and torque will be transmitted to the physics engine to handle the motion of rigid bodies.

5 Rigid Boundary Sampling

In order to optimize the position of sample points, reduce noises and get a uniform distribution set of sampling points, we propose a sampling method with a surface relaxation step. For rigid objects sampling, boundary particles is used to sample the surface of rigid objects, which has several merits. For one thing, using particles can derive a rigid model which can handle different shapes even with complex geometry structure. For another thing, the use of boundary particles successfully alleviates sticking artifacts and makes sampling uniform. As shown in Fig. 2, we first sample the surface of rigid object using the sampling method in [11], then we improve it with surface relaxation (Fig. 1).

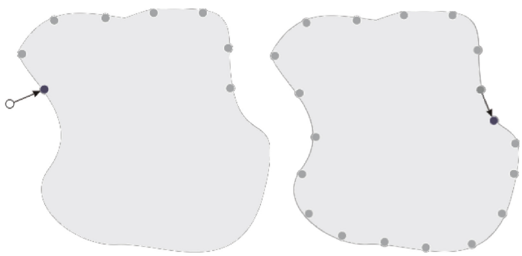

(a) Surface sampling (b) Surface relaxation

Fig. 1. Surface sampling and relaxation. Black points: newly added points. Gray points: Surface sampling points. White points: exterior points before projected to the surface.

Surface relaxation algorithm is presented in Algorithm 1. Unlike using random testing way in [11], we compel particles move by density gradient. It makes particles move to sparse aera, which insures uniform distribution of particles. It starts with the initial sample obtained by surface sampling. Then it computes density $\rho_i(t)$ and density gradient $\nabla\rho_i(t)$ of each surface particles, using deviation of $\rho_i(t)$ and average density

$\overline{\rho_i(t)}$ as a coefficient to tune distance d. Next it employs $d \cdot \nabla\rho_i(t)$ t o adjust particle locations. Surface sample candidates are additionally projected to the surface of the level set and merely reserved which satisfies the Poisson disk criterion. Particle's density gradient using SPH gradient formula which is $<\nabla\rho_i> = \sum_{j=1}^{N} m_j \nabla W(|\mathbf{x}_i - \mathbf{x}_j|, h)$, while projection formula is $\mathbf{p}^{new} = \mathbf{p} + d \cdot \nabla\rho_i(t) - \nabla\phi(\mathbf{p}^{new})$.

Algorithm 1 Surface Relaxation

Input: sample set S , Level set ϕ , radius r , count t , constant f
Output: relaxed sample set S

```
for each t do
  for each p_i ∈ S do
    compute density ρ_i(t), average density ρ̄(t)
    compute density gradient ∇ρ_i(t)
    d ← r · |(ρ_i(t) − ρ̄(t)) / ρ̄(t)| · f
    p^new ← p + d · ∇ρ_i(t)
    if p^new outside φ or came from surface sample
        Project p^new to surface of φ
    if p^new satisfies the Poisson Disk criterion in S
        p ← p^new
```

We compare our method to fast Poisson disk method [11] in a 2 dimension experiment. We randomly generate 100 points in a 0.1×0.1 square and relax it using our method and fast Poisson disk method respectively. Figure 2 shows the relaxation results, the first row is our method and the second row is fast Poisson disk. The column (a) reveals the distribution of points after relaxation and the red point means it do not satisfy Poisson disk condition. Each algorithm iterates 100 times, while column (b) illustrates the number of points that do not satisfy Poisson disk conditions each iteration. It is obvious that our method get a better results with a slight concussion. Besides, our method is more efficient, in matlab environment our method takes 2.44691 s while relaxation fast Poisson disk method costs 56.44153 s for 100 iterations.

6 Implementation and Results

We implemented our method to rigid-fluid coupling animation system and verified the validity of our method. The simulation is performed on an Intel 3.50 GHz CPU with 4 cores. Bullet is used for simulating rigid objects and OpenMP is used for parallelize particle computations. We reconstruct fluid surface using anisotropic kernels [19]. Images were rendered with Blender.

In order to demonstrate the validity of fluid-rigid coupling simulation system, we designed a scene of water shock sculpture using 873 k fluid particles. The experimental

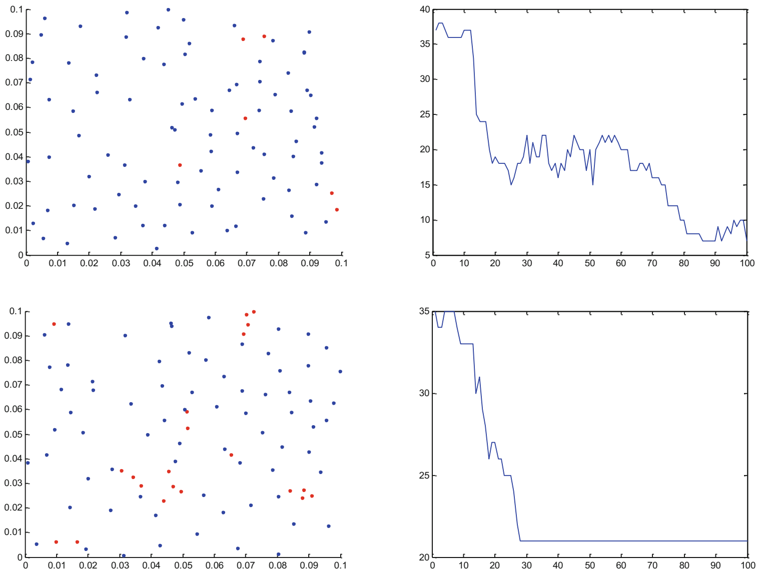

(a) Relaxation results (b) points not conform to the conditions

Fig. 2. Relaxation results comparison of our method with fast Poisson disk.

results are displayed in Fig. 3. In this scenario, the breaking dam of water hit the sculpture which is knocked down and pushed for some distances due to kinetic energy of water. The motions of sculpture are in line with expectations which proved the simulation and calculation of fluid-rigid coupling system accord with physics laws.

The experiments proved our method can implement vivid fluid-rigid coupling animation simulation system with high realistic effects. It can be expected that this animation system can be used to virtual reality domain, special effects in film and game.

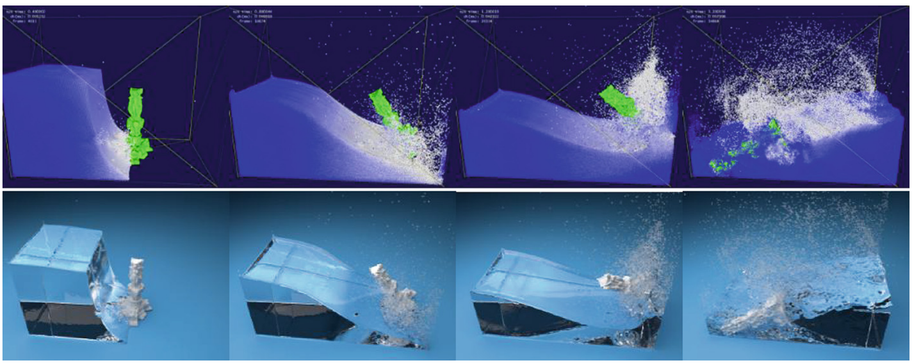

Fig. 3. Water shock sculpture. Top: simulation in particle view; Bottom: rendering results.

7 Conclusion

We proposed an efficient and simple rigid-fluid coupling scheme for particle-based fluid simulation. Our approach samples the surface of rigid bodies with boundary particles that interact with fluids. It insures uniform distribution of particles which requires less iterations. In addition, we combine rigid bodies sampling with boundary handling for rigid-fluid coupling. The scheme is implemented in rigid-body coupling scene which has a good sense of visual reality. Overall, our sampling and coupling method can be applied to other particle-based simulation or relevant approaches. Future work would be extending the method to IISPH and large-scale scenarios.

Acknowledgements. This work was supported by National Natural Science Foundation of China (No. 61272357, 61300074, 61572075).

References

1. Monaghan, J.J.: Simulating free surface flows with SPH. J. Comput. Phys. **110**(2), 399–406 (1994)
2. Muller, M., Charypar, D., Gross, M.: Particle-based fluid simulation for interactive applications. In: Proceedings of the 2003 ACM SIGGRAPH/Eurographics symposium on Computer animation. Eurographics Association, pp. 154–159 (2003)
3. Becker, M., Teschner, M.: Weakly compressible SPH for free surface flows. In: Proceedings of the 2007 ACM SIGGRAPH/Eurographics symposium on Computer animation. Eurographics Association, pp. 209–217 (2007)
4. Solenthaler, B., Pajarola, R.: Predictive-corrective incompressible SPH. ACM Trans. Graph. (TOG) **28**(3), 40 (2009)
5. Ihmsen, M., Cornelis, J., Solenthaler, B., et al.: Implicit Incompressible SPH. IEEE Trans. Vis. Comput. Graph. **20**(3), 426–435 (2014)
6. Bender, J., Koschier, D.: Divergence-free smoothed particle hydrodynamics. In: ACM SIGGRAPH/ Eurographics Symposium on Computer Animation, pp. 147–155. ACM 2015
7. Muller, M., Schirm, S., Teschner, M., Heidelberger, B., Gross, M.: Interaction of fluids with deformable solids. Comput. Animation VirtualWorlds **15**(34), 159–171 (2004)
8. Monaghan, J.J., Kajtar, J.: SPH particle boundary forces for arbitrary boundaries. Comput. Phys. Commun. **180**(10), 1811–1820 (2009)
9. Hu, X., Adams, N.: A multi-phase SPH method for macroscopic and mesoscopic flows. J. Comput. Phys. **213**(2), 844–861 (2006)
10. Ihmsen, M., Akinci, N., Gissler, M., Teschner, M.: Boundary handling and adaptive time-stepping for PCISPH. In: Workshop on Virtual Reality Interaction and Physical Simulation, pp 79–88. The Eurographics Association (2010)
11. Schechter, H., Bridson, R.: Ghost SPH for animating water. ACM Trans. Graph. **31**(4), 611–618 (2012)
12. Akinci, N., Ihmsen, M., Akinci, G., et al.: Versatile rigid-fluid coupling for incompressible SPH. ACM Trans. Graph. (TOG) **31**(4), 62 (2012)
13. Turk, G.: Generating textures on arbitrary surfaces using reaction-diffusion. In: ACM SIGGRAPH Computer Graphics, vol. 25(4), pp. 289–298. ACM (1991)

14. Witkin, A.P., Heckbert, P.S.: Using particles to sample and control implicit surfaces. In: Proceedings of the 21st Annual Conference on Computer Graphics and Interactive Techniques, pp. 269–277. ACM (1994)
15. Cook, R.L.: Stochastic sampling in computer graphics. ACM Trans. Graph. (TOG) **5**(1), 51–72 (1986)
16. Corsini, M., Cignoni, P., Scopigno, R.: Efficient and flexible sampling with blue noise properties of triangular meshes. IEEE Trans. Visual Comput. Graph. **18**(6), 914–924 (2012)
17. Dunbar, D., Humphreys, G.: A spatial data structure for fast Poisson-disk sample generation. ACM Trans. Graph. (TOG) **25**(3), 503–508 (2006)
18. Bridson, R.: Fast poisson disk sampling in arbitrary dimensions. In: ACM SIGGRAPH, p. 5 (2007)
19. Wang, X.K., Ban, X.J., Liu, X., et al.: Efficient extracting surfaces approach employing anisotropic kernels for SPH fluids. J. Vis. **19**(2), 301–317 (2016)